Study of He–H2CO collisions at interstellar temperatures using the L 2 Rmatrix method

C. J. Bocchetta, J. Gerratt, and G. Guthrie

Citation: The Journal of Chemical Physics **88**, 975 (1988); doi: 10.1063/1.454123
View online: http://dx.doi.org/10.1063/1.454123
View Table of Contents: http://scitation.aip.org/content/aip/journal/jcp/88/2?ver=pdfcov
Published by the AIP Publishing

Study of He–H_2CO collisions at interstellar temperatures using the L^2R-matrix method

C. J. Bocchetta, J. Gerratt, and G. Guthrie
Department of Theoretical Chemistry, University of Bristol, Bristol BS8 1TS, United Kingdom

(Received 29 June 1987; accepted 15 September 1987)

Total cross sections for collisions of He(^1S) atoms with H_2CO molecules at interstellar temperatures (18–120 K) have been calculated using the L^2 R-matrix method developed previously. Using 13 slightly nonorthogonal radial basis functions, excellent agreement has generally been obtained with an earlier close-coupled study. However, in two crucial regions (32.7 and 47.7 K) where strong resonances had been reported, we find that the cross sections are smooth. The accuracy of the present calculations were checked at intervals using the de Vogelaere method with parameters set very tightly. Strong resonances in the 20.2 K region were however found and characterized as being of Feshbach (compound state) type, with the He atom lying in the potential well near the O atom of formaldehyde. Similar resonances in the 127 K region are also predicted. Consequently the state-to-state rate constants, upon which the collision pump mechanism for the cooling of the k doublets of formaldehyde depends, now need to be recomputed using the new values for the cross sections. This series of studies shows that the use of slightly nonorthogonal radial basis functions—and which as a result possess arbitrary derivatives at the R-matrix boundary—is the key to the reliable application of this very stable and versatile method to molecular collision problems.

I. INTRODUCTION

In a previous paper (which we refer to as paper I),[1] it was shown that the key to the reliable application of the Wigner L^2 R-matrix method to the study of molecular collisions[2] is the use of slightly nonorthogonal radial basis functions.[3,4] The effect of the nonorthogonality is that the radial functions possess nonzero derivatives at the R-matrix boundary, as well as nonzero amplitudes. Consequently a finite linear combination of them is able to reproduce both the true derivative of the wave function ($d\psi/dR$), as well as the wave function itself at the boundary. Both of these quantities are essential for accurate results. The so-called "Buttle correction"[5] is no longer needed.

The purpose of the present paper is to apply the same method to an important problem in astrophysics: Formaldehyde molecules in dark interstellar clouds are observed in absorption by the k-doublet transitions $1_{10}\leftarrow 2_{11}$ and $2_{11}\leftarrow 2_{12}$, as shown in Fig. 1. However the relative intensities indicate a distribution of the H_2CO molecules among these levels that is characteristic of temperatures not only below the surrounding kinetic temperature (10–20 K), but even below the background temperature ($\sim$2.7 K).[6]

This anomalous cooling of the k doublets can be explained by a collisional pump mechanism with H_2 as the most likely partner.[7,8] A detailed quantum mechanical study of the collisions of H_2CO with He (referred to henceforth as GLM)[9] has generally confirmed this mechanism, and the results are widely used by astrophysicists. At the temperatures considered (<100 K), the H_2 molecules are all in the ground ($v=0, j=0$) state and consequently the He($1s^2;{}^1S$) atom provides a good representation of H_2. This is a considerable advantage, since He–H_2CO collisions (atom + asymmetric top) are very much easier to study than H_2–H_2CO encounters.

A central feature of the GLM result is the indication of strong resonances at $\sim$20.2, 32.7, and 47.7 K. These were not investigated by them in detail, but the existence or otherwise of long-lived collision complexes must have an important bearing on the state-to-state rate constants, and consequently upon the operation of the collisional pump. The R-matrix method is well suited for the investigation of resonances, and this provides the essential motivation for this work.

II. THE ORTHO-FORMALDEHYDE–HELIUM SYSTEM

In order to establish our notation, we begin this section with a brief discussion of the rotational wave functions and energy levels of formaldehyde, treated as a rigid rotor in its $^1A_1$ ground electronic state. We distinguish between two coordinate systems, one fixed in space (the SF system) with coordinate axes labeled x, y, and z, and a body-fixed (BF) system whose axes are directed along the three principal axes a, b, and c of the molecule. The orientation of the BF system with respect to the SF axes is described by three Euler angles α, β, and γ.

The Hamiltonian for a rigid rotor in the BF coordinate system is given by

$$\mathscr{H} = \frac{\hbar^2}{2}\left(\frac{\hat{j}_a^2}{I_a}+\frac{\hat{j}_b^2}{I_b}+\frac{\hat{j}_c^2}{I_c}\right) = A\hat{j}_a^2 + B\hat{j}_b^2 + C\hat{j}_c^2, \tag{2.1}$$

in which I_a, I_b, and I_c are the moments of inertia about the principal axes, and by convention $I_a \leqslant I_b \leqslant I_c$.[10] The rotational constants A, B, and C are simply related to them by

$$A=\hbar^2/2I_a, \quad B=\hbar^2/2I_b, \quad C=\hbar^2/2I_c. \tag{2.2}$$

The operators $\hat{j}_a$, $\hat{j}_b$, and $\hat{j}_c$ are the operators for the compo-

 0021-9606/88/020975-10$02.10

nents of the angular momentum along the indicated axes. The operator for the square of the total angular momentum is related to these by

$$\hat{j}^2 = \hat{j}_a^2 + \hat{j}_b^2 + \hat{j}_c^2 = \hat{j}_x^2 + \hat{j}_y^2 + \hat{j}_z^2. \tag{2.3}$$

Simpler cases occur when $A = B = C$ (spherical top), $A = B \neq C$ (oblate symmetric top), or $A \neq B = C$ (prolate symmetric top). It is obvious that none of these apply to formaldehyde in which all three principal moments of inertia are distinct, so that this molecule is an asymmetric top.

The Hamiltonian (2.1) in this most general case is invariant under rotations by π about each of the principal axes and under inversion of all coordinates. These operations constitute the group D_{2h}, and as a result the eigenfunctions of $\mathscr{H}$ form bases for irreducible representations of this group. In order to determine these eigenfunctions, we consider first the eigenfunctions common to the operators $\hat{j}^2, \hat{j}_c$, and $\hat{j}_z$[12]:

$$\hat{j}^2 D^j_{mk}(\alpha,\beta,\gamma) = j(j+1) D^j_{mk}(\alpha,\beta,\gamma),$$
$$\hat{j}_c D^j_{mk}(\alpha,\beta,\gamma) = k D^j_{mk}(\alpha,\beta,\gamma), \tag{2.4}$$

and

$$\hat{j}_z D^j_{mk}(\alpha,\beta,\gamma) = m D^j_{mk}(\alpha,\beta,\gamma).$$

These functions are the Wigner rotation matrices or D functions. They are eigenfunctions of $\mathscr{H}$ in the simpler cases above, and also provide a suitable basis for expanding the eigenfunctions of $\mathscr{H}$ as follows:

$$\chi^{\mathrm{ASY}}_{jm\tau}(\alpha,\beta,\gamma) = \sum_{k=-j}^{j} a^{j\tau}_{mjk} \phi^{\mathrm{SY}}_{jmks}(\alpha,\beta,\gamma). \tag{2.5}$$

In this expression, the $\phi^{\mathrm{SY}}_{jmks}$ are symmetric top wave functions, suitably symmetrized for D_{2h} symmetry. Thus for $k \neq 0$ we have

$$\phi^{\mathrm{SY}}_{jmks} = \sqrt{1/2}\,(\psi^{\mathrm{SY}}_{jmk} + (-)^s \psi^{\mathrm{SY}}_{jm-k}) \quad (s = 0 \text{ or } 1) \tag{2.6a}$$

and for $k = 0$.

$$\phi^{\mathrm{SY}}_{jmks} = \psi^{\mathrm{SY}}_{jm0}, \tag{2.6b}$$

where

$$\psi^{\mathrm{SY}}_{jmk}(\alpha,\beta,\gamma) = \left(\frac{2j+1}{8\pi^2}\right)^{1/2} D^j_{mk}(\alpha,\beta,\gamma). \tag{2.7}$$

The expansion coefficients $a^{j\tau}_{mjk}$ in Eq. (2.5) are determined by constructing the matrix of the Hamiltonian (2.1) over the functions (2.6) and diagonalizing. The resulting energy levels are characterized by the quantum number j and the index τ, and are $(2j+1)$-fold degenerate in the quantum number m_j. Note that τ also implies a specific value of s.

A more detailed designation of the index τ for the energy levels can be obtained by considering what happens to expansion (2.5) as I_b is gradually decreased to become equal to I_a.[11] In this limit, the molecule is an oblate symmetric top, and only one term in (2.5) survives: that for which k takes on the value k_+, and this is now the unique value of τ. At the other extreme, as I_b is increased to become equal to I_c, the molecule becomes a prolate symmetric top, and the only remaining term in Eq. (2.5) has k equal to k_- say, and this can again be taken as τ. In other words, for a given value of j, each energy level is uniquely associated with two extreme values of k, k_+, and k_-, and these may be used to identify the levels of the asymmetric rotor in the form $j_{k_-k_+}$. We can finally assign an integral index value to τ by defining it as $k_- - k_+$.

In the case of formaldehyde, the rotational constants have been reported by Oka[13] and are

$A = 289\,029$ MHz, $B = 38\,835$ MHz,

$C = 34\,003$ MHz.

It can be seen that $B \simeq C$ so that formaldehyde is close to a prolate symmetric top, and this is reflected in the pattern of the energy levels shown in Fig. 1. The levels occur in closely spaced doublets, corresponding to splitting of the degeneracy $\pm k_-$ in the hypothetical limit $B = C$. A total of 16 states—the same as those used by GLM—were used in the present study. The values of the energy levels are obtained by diagonalizing the Hamiltonian matrix in a basis of symmetric top eigenfunctions as described above, and are listed in Table I.

As a result of the D_{2h} symmetry, the values of k occurring in the expansion (2.5) are either all even or all odd. The wave function $\chi^{\mathrm{ASY}}_{jm\tau s}$ consequently is either unchanged or changes sign on rotation by C_2^a. In the case of formaldehyde

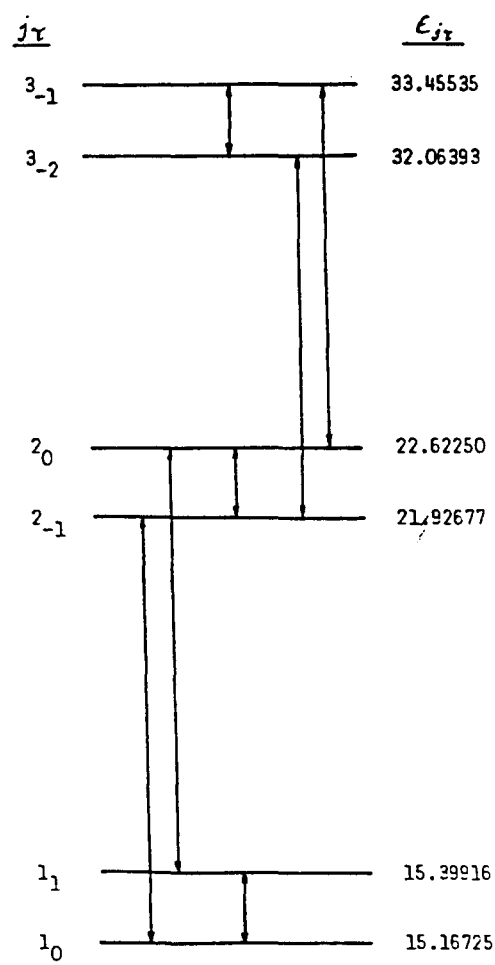

FIG. 1. The lowest six energy levels (in K) for ortho-formaldehyde, with the dipole-allowed transitions shown. Diagram is not to scale.

TABLE I. Energy levels of ortho-formaldehyde. The numbers are those used in the calculation with the significant figures shown.

$j_{k_-k_+}$	$j\tau$	Level	$\epsilon_{j\tau}$ in K
1_{11}	1_0	1	15.167 25
1_{10}	1_1	2	15.399 16
2_{12}	2_{-1}	3	21.926 77
2_{11}	2_0	4	22.622 50
3_{13}	3_{-2}	5	32.063 93
3_{12}	3_{-1}	6	33.455 35
4_{14}	4_{-3}	7	45.576 25
4_{13}	4_{-2}	8	47.895 10
5_{15}	5_{-4}	9	62.460 42
5_{14}	5_{-3}	10	65.938 14
3_{31}	3_2	11	127.063 81
3_{30}	3_3	12	127.063 84
4_{32}	4_1	13	141.053 44
4_{31}	4_2	14	141.053 65
5_{33}	5_0	15	158.543 46
5_{32}	5_1	16	158.544 33

this operation also has the effect of interchanging the two H atoms.

The H_2CO molecules observed in the interstellar gases all have the spins of the two identical nuclei coupled to form a triplet (ortho-formaldehyde).[6] The nuclear spin wave function is therefore unchanged when the two nuclei are interchanged. Since protons satisfy the Pauli principle on permutation of their coordinates, we require that the rotational wave function changes sign under the operation C_2^a. In other words, only states $j\tau$ need to be considered for which k in Eq. (2.5) is odd. Those shown in Table I are the 16 lowest in energy which fulfill this requirement.

The total Hamiltonian for the ortho-H_2CO–He system in a SF coordinate frame is

$$\mathscr{H} = \mathscr{H}(\omega,\mathbf{R}) = \frac{-\hbar^2}{2\mu}\frac{1}{R^2}\frac{\partial}{\partial R}\left(R^2\frac{\partial}{\partial R}\right) + \frac{\hat{l}^2}{2\mu R^2} + \mathscr{H}_T(\omega) + V(\omega,\mathbf{R}). \tag{2.8}$$

In this expression, ω stands for the internal coordinates of the H_2CO target molecule (which in this case are just the three Euler angles mentioned above), and correspondingly $\mathscr{H}_T(\omega)$ denotes the rigid rotor Hamiltonian (2.1). The position of the He atom relative to the center of mass of the H_2CO molecule is denoted by the vector $\mathbf{R}$ which is of length R and has angular coordinates Ω relative to the SF frame. The reduced mass of He–H_2CO is denoted by μ. The radial kinetic energy of the He atom with respect to the center of mass of the formaldehyde target is given by the first term of Eq. (2.8), and the contribution to the total energy from its angular motion about H_2CO is given by the second, where l is the associated angular momentum. The last term in Eq. (2.8) is the potential of interaction between He and H_2CO; it is discussed in detail below.

By combining the wave function for the angular motion of He about H_2CO with that for the rotational motion of the H_2CO target, we obtain the following channel function in the total angular momentum representation[14]:

$$\phi_{j\tau l}^{JM\Pi}(\omega,\Omega) = (2J+1)^{1/2}\sum_{m_j,m_l}(-)^{l-j+M} \times \begin{pmatrix} j & l & J \\ m_j & m_l & -M \end{pmatrix} Y_{lm_l}(\Omega)\chi_{jm_j\tau}^{\mathrm{ASY}}(\omega). \tag{2.9}$$

In this expression $\chi_{jm_j\tau}^{\mathrm{ASY}}$ is the same function as that appearing in Eq. (2.5), and all the other symbols on the right-hand side have their usual meaning. The parity of this function with respect to inversion of all coordinates is denoted by Π and is given by

$$\Pi = (-)^{j+k+s+l} \equiv p_{j\tau}(-)^l,$$

in which the values of k and s are those implied by the index τ, and $p_{j\tau}$ is simply the parity of the $j\tau$ state of H_2CO. A particular channel is thus specified by the quantum numbers $(j\tau l)$, and we shall denote this by the single index c, c', or c_0 whenever possible.

A partial wave for the He–H_2CO system may be written as

$$\psi_{cc_0}^{JM\Pi}(\omega,\mathbf{R}) = \frac{1}{R}F_{cc_0}^{J\Pi}(R)\phi_c^{JM\Pi}(\omega,\Omega), \tag{2.10}$$

in which $c_0 \equiv (j_0\tau_0 l_0)$ may be regarded as the initial state of the system. The radial functions $F_{cc_0}^{J\Pi}(R)$ are determined by the R-matrix procedure (see Sec. III), subject to the boundary conditions:

$$F_{cc_0}^{J\Pi}(R) \equiv F_{j\tau l;j_0\tau_0 l_0}^{J\Pi}(R)$$

$$\underset{R\to\infty}{\to} \delta_{cc_0}h_l^-(k_{j_0\tau_0}R) - \left(\frac{k_{j_0\tau_0}}{k_{j\tau}}\right)^{1/2}h_l^+(k_{j\tau})S_{j\tau l;j_0\tau_0 l_0}^{J\Pi}, \quad (k_{j\tau}\geqslant 0; k_{j_0\tau_0}\geqslant 0), \tag{2.11a}$$

$$\underset{R\to\infty}{\to} \exp(-|k_{j\tau}|R) \quad (k_{j\tau}<0; k_{j_0\tau_0}\geqslant 0), \tag{2.11b}$$

$$\underset{R\to\infty}{\to} \exp(-|k_{j_0\tau_0}|R) \quad (k_{j_0\tau_0}<0). \tag{2.11c}$$

In these expressions, the functions $h_l^{\pm}(x)$ are the Riccati–Hankel functions,[15] and $S_{cc_0}^{J\Pi}$ is an element of the collision matrix. All radial functions are required to be regular at the origin. The magnitude of the wave vector $k_{j\tau}$ is given by

$$k_{j\tau}^2 = 2\mu(E-\epsilon_{j\tau})/\hbar^2, \tag{2.12}$$

where E is the total energy of the He–H_2CO system relative to He and H_2CO at rest in their ground states, and $\epsilon_{j\tau}$ is the energy of the formaldehyde molecule in the specified state. The total wave function for the He–H_2CO system is written as

$$\psi_{c_0}(\omega,\mathbf{R}) = \sum_{J,M,\Pi}\sum_c \frac{1}{R}F_{cc_0}^{J\Pi}(R)\phi_c^{JM\Pi}(\omega,\Omega). \tag{2.13}$$

Each term in this gives rise to a partial collision cross section,

$$\sigma_{j\tau\leftarrow j_0\tau_0}^{J\Pi}(E) = \frac{\pi(2J+1)}{k_{j\tau}^2(2j_0+1)}$$

$$\times \sum_{l=|J-j|}^{J+j} \sum_{l_0=|J-j_0|}^{J+j_0} |S^{J\Pi}_{j\tau l;j_0\tau_0 l_0} - \delta_{jj_0}\delta_{ll_0}\delta_{\tau\tau_0}|^2, \tag{2.14}$$

and the total cross section is just

$$\sigma_{j\tau\leftarrow j_0\tau_0}(E) = \sum_{J,\Pi} \sigma^{J\Pi}_{j\tau\leftarrow j_0\tau_0}(E). \tag{2.15}$$

The potential energy of interaction between the He and H_2CO, $V(\omega,\mathbf{R})$, is expanded in the form

$$V(\omega,\mathbf{R}) = \sum_{\lambda,\mu,\nu} \left(\frac{4\pi}{2\lambda+1}\right)^{1/2} v_{\lambda\mu}(R) D^{\lambda}_{\nu\mu}(\omega) Y_{\lambda\nu}(\Omega). \tag{2.16}$$

This form is convenient for computing matrix elements of V between channel functions (2.9) which are needed in both the inner and outer regions in the R-matrix calculation. These are given by[9]

$$\langle j'\tau' l';J'\Pi'|V|j\tau l;J\Pi\rangle = \delta_{JJ'}\delta_{\Pi\Pi'}(-)^{j+j'-J} \sum_{k=-j}^{j} \sum_{k'=-j'}^{j'} a^{j\tau}_{mjk} a^{j'\tau'}_{m'j'k'} (-)^{k'} \sum_{\lambda} v_{\lambda,k'-k}(R)$$

$$\times [(2j+1)(2j'+1)(2l+1)(2l'+1)]^{1/2} \begin{pmatrix} l & l' & \lambda \\ 0 & 0 & 0 \end{pmatrix} \begin{pmatrix} j & j' & \lambda \\ k & -k' & k'-k \end{pmatrix} \begin{Bmatrix} j & l & J \\ l' & j' & \lambda \end{Bmatrix}$$

$$= \delta_{JJ'}\delta_{\Pi\Pi'} \sum_{k,k',\lambda} v_{\lambda,k'-k}(R) \mathcal{L}(\lambda;j\tau(k)l;j'\tau'(k')l';J\Pi). \tag{2.17}$$

The potential used is the *ab initio* surface of Garrison *et al.*[16,17] It consists of a sum of an SCF contribution plus correlation terms. A total of 49 terms is included in the summation over λ and μ in Eq. (2.16). The form of the radial terms $v_{\lambda\mu}(R)$ from the SCF treatment is

$$v^{\mathrm{SCF}}_{\lambda\mu}(R) = Ae^{-BR} - C/R^6 - D/R^7$$

$$(0 \leqslant R \leqslant 10.5\, a_0). \tag{2.18}$$

For $R > 10.5\, a_0$, $v^{\mathrm{SCF}}_{\lambda\mu}(R) \equiv 0$. The required A, B, C, and D coefficients for each value of λ and μ are given in Table I of Ref. 9. [It is worth noting that there is a printing error in Eq. (26) of this paper: The R^{-2} terms should be replaced by R^{-7}.] Correlation contributions to the $v_{\lambda\mu}(R)$ are added for $\lambda = 0$, 1, 2, and $\mu = 0$. These are of the form

$$v^{\mathrm{corr}}_{00}(R) = \{\alpha_1 e^{-\beta_1 R} + 4\alpha_2 e^{-\beta_2 R} + \alpha_3 e^{-\beta_3 R} - (\gamma_1 + 4\gamma_2 + \gamma_3)/R^6\}/6,$$

$$v^{\mathrm{corr}}_{10}(R) = \{\alpha_1 e^{-\beta_1 R} - \alpha_3 e^{-\beta_3 R} - (\gamma_1 - \gamma_3)/R^6\}/2,$$

$$v^{\mathrm{corr}}_{20}(R) = \alpha_1 e^{-\beta_1 R} - 2\alpha_2 e^{-\beta_2 R} + \alpha_3 e^{-\beta_3 R} - (\gamma_1 - 2\gamma_2 + \gamma_3)/R^6\}/3. \tag{2.19}$$

The values of the coefficients are:

$\alpha_1 = -1.305\,29 \times 10^4$; $\beta_1 = 0.808\,63$;
$\gamma_1 = 8.197\,53 \times 10^4$,
$\alpha_2 = -5.582\,37 \times 10^4$; $\beta_2 = 1.116\,06$;
$\gamma_2 = 2.088\,46 \times 10^5$,
$\alpha_3 = -8.001\,65 \times 10^4$; $\beta_3 = 1.019\,91$;
$\gamma_3 = 3.461\,52 \times 10^6$.

This form of the potential includes the dipole-induced dipole and dispersion contributions in the long range, both of which vary as R^{-6}, plus a quadrupole-field gradient induction contribution, which varies as R^{-7}. The potential is shown in Fig. 2. Its main feature is the existence of a hemispherical well around the oxygen atom of depth 30 K at a distance of $\sim 7.5\, a_0$ from this atom. There is a similar well around the CH_2 end of the molecule, but this can only be accessed if the He atom approaches perpendicularly to the plane of the H_2CO.

III. THE *R*-MATRIX CALCULATIONS. PRELIMINARY DISCUSSION

The R-matrix calculations were carried out as described in paper I. The inner or "strong interaction" region was defined to range from $R_0 = 4.5\, a_0$ to $A = 10.5\, a_0$. Radial basis functions were generated from the following effective Hamiltonian [cf. Eq. (II.36) of I]:

$${}^0\mathcal{H}^{J\Pi} = \frac{-\hbar^2}{2\mu}\left(\frac{d^2}{dR^2} - \frac{J(J+1)}{R^2}\right) + {}^0V^{J\Pi}_{j\tau j\tau}(R) \tag{3.1}$$

in which the effective potential ${}^0V^{J\Pi}_{j\tau j\tau}(R)$ is the average value of V when the target H_2CO molecule is in state $j\tau$, and the orbital angular momentum l is equal to J:

$${}^0V^{J\Pi}_{j\tau j\tau}(R) \equiv \langle j\tau J;J\Pi|V|j\tau J;J\Pi\rangle = \sum_{k,k',\lambda} v_{\lambda,k'-k}(R) \times \mathcal{L}[\lambda;j\tau(k)J;j\tau(k')J;J\Pi]. \tag{3.2}$$

The value of J was fixed at 10. The parity Π is -1 for target states 1, 4, 5, 8, 9, 11, 14, and 15, and equal to $+1$ for states 2, 3, 6, 7, 10, 12, 13, and 16. The values of the $\mathcal{L}$ coefficients used in Eq. (3.2) which are necessary to define the effective potential are given in Table II. These are input directly into the program as the array ZFAC. Several of the effective potentials are shown in Fig. 3.

The radial basis functions are eigenfunctions of the operator

$${}^0\mathcal{H}^{J\Pi} + L^{J\Pi}_b, \tag{3.3}$$

where the Bloch operator[18] is given by

$$L^{J\Pi}_b = \left(\frac{-\hbar^2}{2\mu}\right)\delta(R-A) \sum_c |\Phi^{JM\Pi}_c(\omega,\Omega)$$

$$\times\frac{\partial}{\partial R}\left[\Phi_c^{JM\Pi}(\omega,\Omega)\right]|. \tag{3.4}$$

The arbitrary constant b_c which normally occurs in $L_b^{J\Pi}$ is put to zero. Solutions $\zeta_{j\tau,n}^{J}(R)$ of Eq. (3.3) are found by forming the matrix of ${}^0\mathscr{H}^{J\Pi}+L_b^{J\Pi}$ in a basis of "primitive sine functions"

$$\chi_k(R)=[2/(A+\delta-R_0)]^{1/2}\times\sin[(k+\tfrac{1}{2})\pi(R-R_0)/(A+\delta-R_0)] \tag{3.5}$$

and diagonalizing.[1,2] Functions (3.5) are orthonormal in the interval $(R_0,A+\delta)$ with zero derivatives at the outer boundary, $R=A+\delta$. A total of 75 such sine functions were included, and the 13 solutions of lowest energy were used for each target state $j\tau$ as the radial basis functions $\zeta_{j\tau,n}^{J}(R)$. A value of $\delta=0.35\,a_0$ was chosen for this purpose. This is the smallest value which gives at least two significant figure agreement with the de Vogelaere method for the partial cross sections for $J=1$ (see discussion in Sec. V).

The R-matrix calculations were carried out using the 13 basis functions in the range (R_0,A). Consequently the $\zeta_{j\tau,n}^{J}(R)$ functions possess nonzero derivatives at $R=A$, and are slightly nonorthogonal. No Buttle correction was used.[5] The results are shown in Tables III–VI where they are also compared with those obtained by GLM.

The calculations were carried out on an IBM 3081 computer, and required 35–40 min per partial wave for the initial calculation (computation of R-matrix eigenvalues and reduced widths), and up to 60 s per partial cross section per energy thereafter (but see below). There is a maximum of 62 coupled channels in this problem. When combined with the 13 radial basis functions, this gives rise to Hamiltonian matrices of maximum dimension 806×806 to be diagonalized. A total of 16 partial waves is needed for convergence.

The calculations in the outer region ($R\geqslant10.5\,a_0$) were carried out by means of the R-matrix propagator technique,[19] using the following setting of the parameters:

$$\text{BETA}=0.18,\quad \text{FACT}=5.00,\quad \text{CUPMAX}=0.05.$$

With these, 50–60 steps were needed to reach the asymptotic region, which was generally found to be at $\sim83\,a_0$. All the computer time at different energies—i.e., the 60 s mentioned above—is taken up at this stage. Since the potential in the outer region is of the form $-C/R^6-D/R^7$ [see Eqs. (2.18) and (2.19)], use of an asymptotic expansion method would reduce the time needed to practically nil.[20,21]

As can be seen from Table III, the first and most important observation to be made at this point is that for total energies in the range corresponding to 30.1668–37.6668 K there is nearly perfect agreement between the R-matrix and coupled channel results for the total cross sections. At high energies, 40.1668–70.1668 K, there is a slight deterioration in the agreement: At 70.1668 K, the differences are on average 10%. Assuming that the coupled channel results are the more accurate, it can be seen that in the R-matrix calculations there is a tendency for transitions between states with high target energy levels—where the changes in the kinetic energy are small—to be least in error.

However the most important conclusion to be drawn concerns the resonant behavior reported by GLM at total energies 20.1668, 32.6668, and 47.6668 K. The energy range 30.5–34 K was examined in steps of 0.5 K. This covers the threshold region of the H_2CO doublets 3_{13} and 3_{12} which occur at 32.063 93 and 33.455 35 K, respectively. No resonant structure was found. The results are shown in Table IV. Furthermore if the present R-matrix results for the total

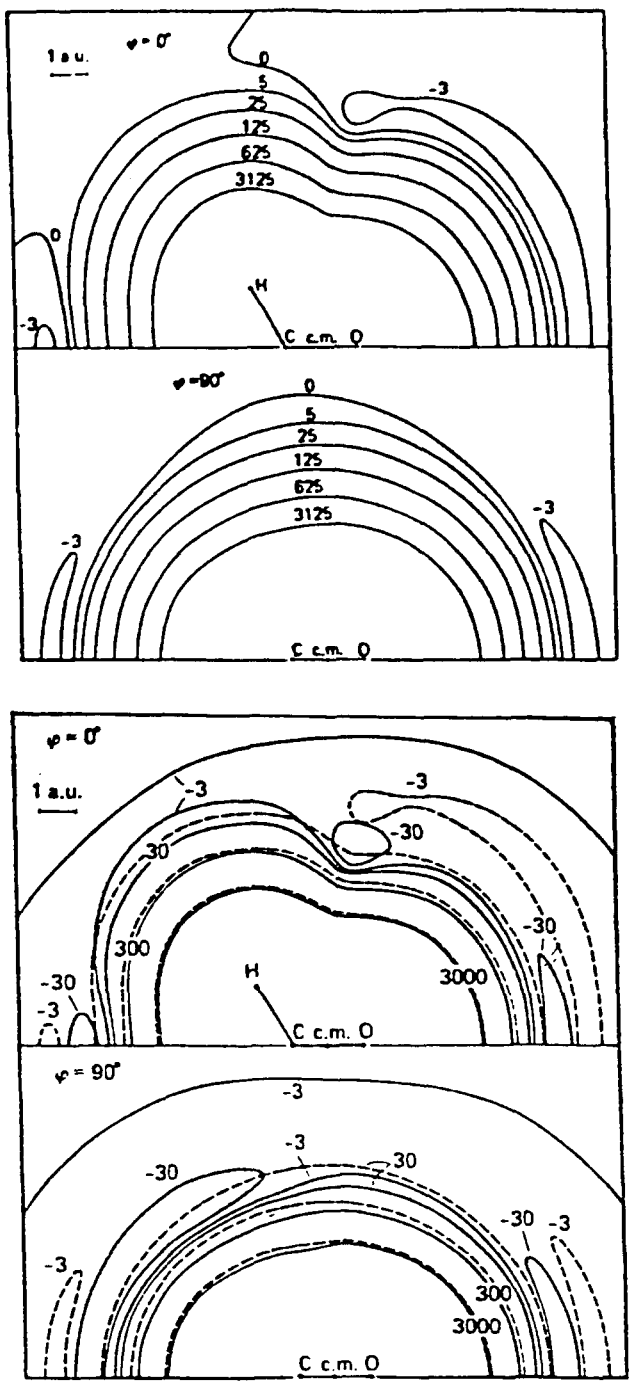

FIG. 2. The top diagram (taken from Garrison *et al.*, Ref. 16) shows a contour plot of the Hartree–Fock interaction potential for He incident in the plane of H_2CO ($\phi=0°$, top panel), and He incident in the bisector plane ($\phi=90°$, bottom panel). The bottom diagram (taken from Garrison, *et al.*, Ref. 17) shows a plot of the Hartree–Fock interaction potential (- - - line) and of the Hartree–Fock + CI potential (— line), for the He incident in the plane of H_2CO ($\phi=0°$, top panel), and for He incident in the bisector plane ($\phi=90°$, bottom panel). All energies are in K.

cross sections in this region are inserted into Table III, we see no significantly anomalous result: The cross sections show a smooth nonresonant behavior. Since 50% of the total cross section is carried by the $J = 4$ partial wave in this energy range, the behavior of the corresponding partial cross section was also further examined in steps of 0.01 K—with the same result.

Nevertheless, more detailed examination of the cross sections in this region does show interesting structure. Table V shows results for the elastic cross sections $\sigma^J_{3_{12}\leftarrow 3_{12}}$, and Tables VI for the inelastic cross sections $\sigma^J_{3_{13}\leftarrow 3_{12}}$. It can be seen at once that virtually the entire cross section at 33.5 K arises from the $J = 3$ partial wave for both parities. This is particularly striking in the elastic case. A H_2CO–He state is clearly present for $J = 3$, although its lifetime is such as not to give rise to any dramatic variation in the total cross section. Because this phenomenon involves H_2CO states where $j = 3$, as well as $J = 3$, it is tempting to conclude that this is a Feshbach[22] type of compound state. However for reasons explained below we believe that this state is in fact more likely to be a kind of shape resonance: With these values of j and J, l may range from 0–6, and its most probable value is 3. Consequently there will be centrifugal barrier, which is the essential prerequisite for this kind of state.

Similar remarks apply to the cross sections in the region of 47.7 K. No resonance structure was found, again in disagreement with GLM (see Table IV)—though it should be added that this region was less thoroughly examined. Nevertheless we are reasonably certain that there are no Feshbach resonances in this region (see Sec. IV).

IV. RESONANCES IN He–H_2CO COLLISIONS

Finally the region near 20.2 K was examined and strong resonances were indeed found. These are shown for partial waves $J = 6$ and $J = 5$ in Figs. 4 and 5 for elastic and inelastic cross sections involving states 1_{11} and 1_{10}.

TABLE II. Values of the f coefficients used in the effective potential equation (3.2).

λ	μ	$1_0(1)$	$1_1(2)$	$2_{-1}(3)$	$2_0(4)$
0	0	2.821×10^{-1}	2.821×10^{-1}	2.821×10^{-1}	2.821×10^{-1}
2	0	6.308×10^{-2}	6.308×10^{-2}	-4.382×10^{-2}	-4.382×10^{-2}
2	2	-1.545×10^{-1}	1.545×10^{-1}	-1.073×10^{-2}	1.073×10^{-2}
4	0			-5.976×10^{-2}	-5.976×10^{-2}
4	2			9.448×10^{-2}	-9.448×10^{-2}
λ	μ	$3_{-2}(5)$	$3_{-1}(6)$	$4_{-3}(7)$	$4_{-2}(8)$
0	0	2.821×10^{-1}	2.821×10^{-1}	2.821×10^{-1}	2.821×10^{-1}
2	0	-5.874×10^{-2}	-5.874×10^{-2}	-6.102×10^{-2}	-6.102×10^{-2}
2	2	-9.652×10^{-2}	9.534×10^{-2}	-8.927×10^{-2}	8.655×10^{-2}
4	0	8.187×10^{-3}	8.187×10^{-3}	1.734×10^{-2}	1.734×10^{-2}
4	2	5.121×10^{-2}	-5.235×10^{-2}	3.624×10^{-2}	-3.687×10^{-2}
6	0	5.290×10^{-2}	5.290×10^{-2}	1.277×10^{-3}	1.277×10^{-3}
6	2	-7.245×10^{-2}	7.209×10^{-2}	-2.565×10^{-2}	2.681×10^{-2}
8	0			-4.503×10^{-2}	-4.503×10^{-2}
8	2			5.750×10^{-2}	-5.665×10^{-2}
λ	μ	$5_{-4}(9)$	$5_{-3}(10)$	$3_2(11)$	$3_3(12)$
0	0	2.821×10^{-1}	2.821×10^{-1}	2.821×10^{-1}	2.821×10^{-1}
2	0	-5.878×10^{-2}	-5.878×10^{-2}	9.791×10^{-2}	9.791×10^{-2}
2	2	-8.215×10^{-2}	7.774×10^{-2}		
4	0	-1.518×10^{-2}	1.518×10^{-2}	2.456×10^{-2}	2.456×10^{-2}
4	2	2.400×10^{-2}	-2.400×10^{-2}		
6	0	-1.912×10^{-3}	-1.912×10^{-3}	3.528×10^{-3}	3.528×10^{-3}
6	2	-6.362×10^{-3}	6.715×10^{-3}		
6	6			-1.072×10^{-1}	1.072×10^{-1}
8	2	4.308×10^{-3}	-4.593×10^{-3}		
10	0	3.626×10^{-2}	3.626×10^{-2}		
10	2	-4.455×10^{-2}	4.325×10^{-2}		
10	4	1.147×10^{-3}	-1.189×10^{-3}		
λ	μ	$4_1(13)$	$4_2(14)$	$5_0(15)$	$5_1(16)$
0	0	2.821×10^{-1}	2.821×10^{-1}	2.821×10^{-1}	2.821×10^{-1}
2	0	2.512×10^{-2}	2.512×10^{-2}	-6.543×10^{-3}	-6.544×10^{-3}
2	2	1.337×10^{-3}	1.388×10^{-3}	1.848×10^{-3}	1.970×10^{-3}
4	0	-4.046×10^{-2}	-4.045×10^{-2}	-2.277×10^{-2}	-2.77×10^{-2}
6	0	-2.175×10^{-2}	-2.175×10^{-2}	4.623×10^{-3}	4.623×10^{-3}
6	6	-3.889×10^{-2}	3.889×10^{-2}	-9.692×10^{-3}	9.692×10^{-3}
8	0	-6.436×10^{-3}	-6.444×10^{-3}	4.573×10^{-3}	4.573×10^{-3}
8	6	6.661×10^{-2}	-6.661×10^{-2}	5.191×10^{-3}	-5.191×10^{-3}
10	0			7.778×10^{-3}	7.779×10^{-3}
10	4			-1.147×10^{-3}	1.189×10^{-3}
10	6			-4.798×10^{-2}	4.798×10^{-2}

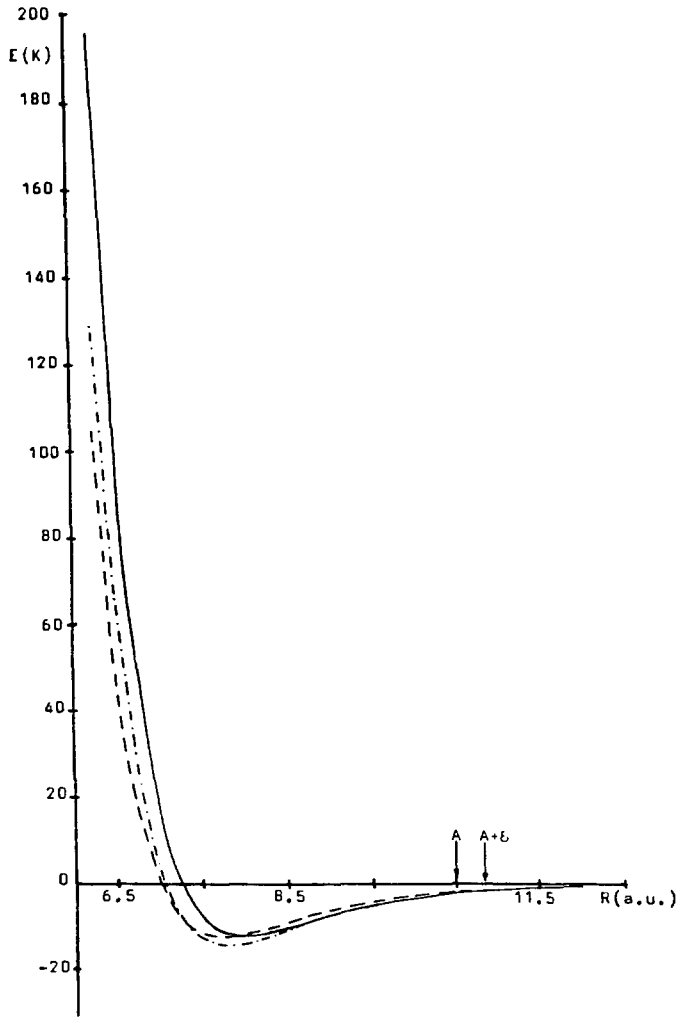

FIG. 3. The diagram shows various potentials used in the effective Hamiltonians. The curves support bound states at approximately -3 K. The arrows indicate the position of the R-matrix boundary ($A = 10.5\,a_0$), and the region defining the radial functions $\zeta_{j\tau,n}(R)$ ($A + \delta = 10.85\,a_0$).

Before discussing these findings, an important result of paper I must be recalled. The behavior of the reduced widths $\gamma_{\lambda c}$ for fixed channel c as a function of the R-matrix level ϵ_λ is an excellent indicator of resonances involving that channel. For values of λ corresponding to energies ϵ_λ well below threshold for channel c, the $\gamma_{\lambda c}$ are very small: $\sim 10^{-6}$. As λ approaches threshold from below, and if resonances are present, $\gamma_{\lambda c}$ suddenly increases in absolute value by a factor of $\sim 10^4$. This provides a sensitive criterion for the presence of even the narrowest resonances. However it should be noted that essentially this constitutes a test for Feshbach resonances. Shape resonances will not be detected by this procedure unless the entire barrier is included in the strong interaction region—which is not the case here.

For the simple atom–diatom collinear problem of I it was possible to carry out this test by eye. In the present case the file of reduced widths $\gamma^J_{\lambda c}$ contains $\sim 10^4$ entries, and a small program was written to scan it and detect this pattern.

When applied to the 32.7 and 47.7 K regions, the test proved negative. This provides strong evidence that the unusual behavior of the $J = 3$ partial wave at 33.5 K concerns a state arising from penetration through a centrifugal barrier.

However in the 20.2 K region we find that the pattern of reduced widths indicates resonances at energies just below the threshold for excitation of the 2_{12} and 2_{11} states of H_2CO. There is an obvious distinction between the parities in the elastic case: The resonant structure of the 1_{10}–1_{10} cross section arises entirely from the He–H_2CO states of parity ($-$), while both parities contribute to the inelastic case. The number and close spacing of the calculated energy points should

TABLE III. State-to-state total cross sections (Å^2) obtained from R-matrix, close-coupled and coupled state calculations for the total energies shown (in K). (1) L^2 R-matrix result; (2) close-coupled; (3) coupled states.

$j\tau \to j'\tau'$		30.1668 K			35.1668 K			37.6668 K		
		(1)	(2)	(3)	(1)	(2)	(3)	(1)	(2)	(3)
1	1	213	213	215	189	189	194	179	179	187
1	2	15.1	15.1	18.0	12.3	12.3	14.1	11.5	11.5	12.3
1	3	23.2	23.3	20.9	20.3	20.2	19.9	18.1	18.1	18.0
1	4	13.9	13.9	3.1	11.2	11.2	6.7	9.5	9.5	7.3
1	5				4.1	4.1	2.9	5.4	5.4	4.0
1	6				0.3	0.3	0.2	0.6	0.6	0.3
2	2	230	231	220	194	194	204	182	182	194
2	3	15.6	15.4	11.6	11.5	11.5	11.8	9.9	9.9	11.6
2	4	16.0	16.0	7.8	14.4	14.3	9.2	12.4	12.4	8.7
2	5				7.6	7.6	3.8	8.6	8.6	5.8
2	6				1.5	1.6	0.9	2.3	2.4	1.1
3	3	249	249	253	217	217	214	205	205	201
3	4	19.8	19.9	21.1	13.2	13.1	12.9	10.4	10.4	11.1
3	5				11.8	11.9	9.7	13.3	13.3	12.6
3	6				2.1	2.1	1.4	3.3	3.3	2.0
4	4	263	263	289	229	229	244	212	211	221
4	5				7.0	7.1	4.4	7.9	7.9	5.2
4	6				8.1	8.2	6.1	11.6	11.5	10.8
5	5				289	289	252	277	277	263
5	6				9.6	9.6	16.1	10.2	10.2	12.2
6	6				253	253	176	288	288	282
$j\tau \to j'\tau'$		40.1668 K			42.6668 K			70.1668 K		
		(1)	(2)	(3)	(1)	(2)	(3)	(1)	(2)	(3)
1	1	175	170	178	166	163	169	120	115	118
1	2	10.8	11.1	11.7	10.0	10.1	10.7	7.0	7.6	6.9
1	3	16.8	17.1	17.3	16.4	16.7	17.2	10.2	10.5	11.3
1	4	8.7	8.9	8.1	7.7	8.0	8.5	5.6	5.7	7.3
1	5	6.2	6.3	4.3	6.4	6.4	4.4	4.8	5.4	4.3
1	6	0.8	0.8	0.3	1.2	1.2	0.3	1.4	0.9	0.7
2	2	176	174	185	168	167	177	122	115	118
2	3	9.5	9.7	11.4	8.8	9.2	11.5	5.9	6.3	9.0
2	4	11.6	11.6	8.7	10.3	10.3	8.1	9.3	8.4	7.4
2	5	7.7	7.6	6.3	7.3	7.2	6.3	4.8	4.7	4.9
2	6	2.7	2.6	1.0	3.6	3.7	1.1	5.0	4.5	3.2
3	3	198	197	190	188	186	182	125	122	121
3	4	8.4	8.4	9.5	7.3	7.1	8.4	3.5	3.5	3.9
3	5	13.5	13.3	13.0	13.8	12.9	12.4	11.4	11.6	11.7
3	6	3.5	3.7	2.3	3.8	3.7	2.1	4.0	3.4	2.7
4	4	205	204	207	197	195	198	130	124	126
4	5	6.6	6.8	5.5	6.9	7.3	5.7	3.8	3.7	4.1
4	6	12.3	12.1	10.4	10.8	10.4	10.1	8.4	9.5	8.9
5	5	253	255	239	240	244	233	127	135	131
5	6	8.6	8.8	9.4	8.9	9.2	7.7	2.8	2.8	3.0
6	6	294	293	266	281	281	266	142	142	142

TABLE IV. State-to-state total cross sections in Å^2 obtained by R-matrix and close-coupled methods at the resonance energies (degrees K) of GLM. No resonant features are observed when using the R-matrix method. If the R-matrix results are inserted in the appropriate places a smooth nonresonant behavior is seen. (1) L^2 R-matrix result; (2) close-coupled.

		32.6668 K		47.6668 K	
$j\tau\rightarrow j'\tau'$		(1)	(2)	(1)	(2)
1	1	198	345	154	152
1	2	12.8	45.5	9.4	9.5
1	3	22.0	37.6	14.1	16.1
1	4	13.6	17.1	7.1	7.7
1	5	1.1	4.8	5.6	8.0
1	6			1.3	1.6
1	7			1.6	3.0
2	2	206	418	155	154
2	3	13.7	33.1	8.2	8.5
2	4	16.7	34.9	9.3	8.9
2	5	1.9	2.5	6.8	7.0
2	6			4.1	4.7
2	7			2.0	3.0
3	3	232	430	171	178
3	4	18.3	92.4	5.6	5.5
3	5	4.0	10.8	12.8	20.0
3	6			4.9	9.5
3	7			1.1	4.2
4	4	253	414	180	187
4	5	2.7	7.6	5.6	12.3
4	6			13.0	20.2
4	7			2.7	4.2
5	5	235	1620	205	259
5	6			7.8	25.0
5	7			7.8	14.1
6	6			230	353
6	7			3.5	12.7
7	7			255	950

TABLE V. $\sigma^J_{6\rightarrow 6}$ in Å^2 for differing total J and total energies in K for the two parities, obtained by the L^2 R-matrix method.

$J(-)$	33.5	34.0	34.5	35.1668	37.6668	40.1668
0	0.00	0.00	0.01	0.11	1.17	1.53
1	0.00	0.13	1.70	4.93	9.25	6.30
2	0.09	15.7	27.7	30.0	18.4	10.3
3	300.8	140.2	69.8	33.5	31.8	27.6
4	0.25	29.4	55.2	59.4	27.5	24.4
5	0.00	1.24	7.99	19.7	42.3	27.1
6	0.00	0.08	1.19	4.75	21.8	36.1
7	0.00	0.01	0.18	6.60	13.0	18.1
8	0.00	0.00	0.01	0.04	10.0	17.2
9	0.00	0.00	0.00	0.01	0.18	3.69
10	0.00	0.00	0.00	0.00	0.02	0.20
$J(+)$						
0	...	...	...	...	...	...
1	0.00	0.00	0.10	0.69	4.30	4.72
2	0.00	1.03	4.76	10.2	14.7	9.16
3	1.08	43.6	53.6	48.9	19.4	18.3
4	0.00	3.84	13.1	22.9	33.8	20.6
5	0.00	0.55	3.61	10.1	21.4	31.9
6	0.00	0.00	0.06	0.99	16.0	17.3
7	0.00	0.00	0.00	0.02	2.82	17.3
8	0.00	0.00	0.00	0.00	0.10	1.67
9	0.00	0.00	0.00	0.00	0.01	0.11
10	0.00	0.00	0.00	0.00	0.00	0.02

TABLE VI. $\sigma^J_{6\rightarrow 5}$ in Å^2 for differing total J and varying total energies in K for the two parity cases, obtained by the L^2 R-matrix method.

$J(-)$	33.5	34.0	34.5	35.1668	37.6668	40.1668
0	...	...	...	...	...	...
1	0.00	0.03	0.31	0.20	0.06	0.03
2	0.11	0.30	0.33	0.29	0.41	0.19
2	23.3	3.99	2.43	1.84	1.32	0.75
4	0.43	5.88	7.51	5.40	1.25	1.26
5	0.01	0.11	0.13	0.36	2.66	1.04
6	0.00	0.14	0.57	0.55	0.33	1.39
7	0.00	0.00	0.00	0.13	0.51	0.23
8	0.00	0.00	0.00	0.00	0.02	0.26
9	0.00	0.00	0.00	0.00	0.00	0.00
10	0.00	0.00	0.00	0.00	0.00	0.00
$J(+)$						
0	...	...	...	...	...	...
1	0.00	0.03	0.07	0.10	0.06	0.02
2	0.01	0.09	0.11	0.27	0.26	0.19
3	1.57	8.95	7.91	3.51	1.09	0.86
4	0.17	1.20	0.96	0.93	2.66	1.09
5	0.00	1.29	4.09	3.69	0.86	1.72
6	0.00	0.00	0.01	0.08	1.92	0.78
7	0.00	0.00	0.00	0.00	0.07	0.54
8	0.00	0.00	0.00	0.00	0.01	0.03
9	0.00	0.00	0.00	0.00	0.00	0.00
10	0.00	0.00	0.00	0.00	0.00	0.00

be noted. The small "blip" seen at a single energy in the $(+)$ parity contribution to $\sigma_{1_{11}\rightarrow 1_{11}}$ in Fig. 4 is almost certainly due to the positioning of the R-matrix boundary underneath a centrifugal barrier where the amplitude of the wave function becomes very small.

The stability of complexes of the 2_{12} and 2_{11} states of H_2CO with He can be understood as follows: The most stable position for the He atom in the potential well surrounding the oxygen atom of H_2CO is along the C–O axis. Formaldehyde is almost a prolate symmetric top and for the purpose

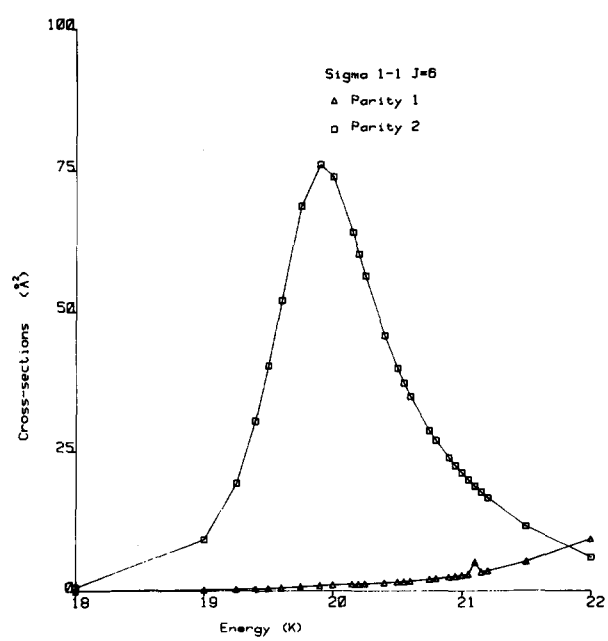

FIG. 4. The resonance at ~20.2 K. $J = 6$ partial wave for $\sigma_{1_{11}\rightarrow 1_{11}}$.

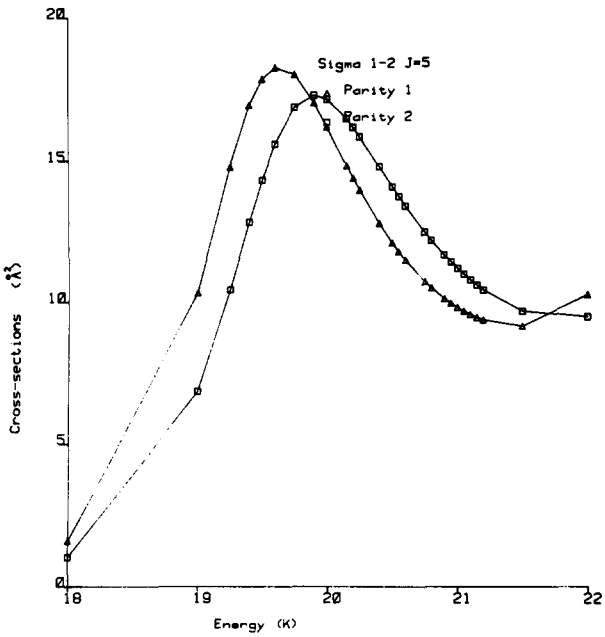

FIG. 5. The resonance at ~20.2 K. $J = 5$ partial wave for $\sigma_{1_{10}-1_{11}}$.

of this discussion we treat it as such. If the H_2CO molecule were to rotate exactly about the C–O axis, the position of the He atom would always remain stable. The more the direction of j differs from that of k_-, the component of j along the C–O axis, the more H_2CO wobbles and consequently the He atom tends to be thrown off.

The situation may be likened to a ball bearing in a cup. When the cup spins smoothly about its vertical axis of symmetry, the ball bearing remains at rest. But if we swirl the cup, the ball bearing is displaced and climbs up the rim. Eventually if the eccentricity of the motion of the cup becomes large enough, the ball bearing flies out.

The 2_{12} and 2_{11} states ($j = 2$, $k = 1$) have the least eccentricity of the low-lying states, and hence are the only ones capable of forming long-lived complexes. Only the 3_{31} and 3_{30} states have smaller eccentricities, but these lie at ~127.064 K—a region which we have not investigated in this study. We predict that these also will give rise to strong Feshbach resonances.

V. FINAL REMARKS

We have studied collisions of He(^1S) atoms with H_2CO molecules at interstellar temperatures using the L^2 R-matrix method developed previously. Using just 13 slightly nonorthogonal radial basis functions, we have generally obtained excellent agreement with a previous close-coupled study. However in two crucial regions where GLM report strong resonances, we find that the cross sections are smooth—although in one case there is indeed unusual behavior reminiscent of a shape resonance. The source of this disagreement is almost certainly the integration method[24] used in the GLM study, which suffers from numerical instability when closed channels are present. We did in fact attempt to repeat the GLM work by using the same algorithm, but found such difficulty in starting off the integration that we finally abandoned it.

It should be stressed that hitherto the central problem with the application of the L^2 R-matrix method to molecular collisions has been lack of convergence in the radial basis functions—and this gives rise to spurious resonances. This series of studies shows that the use of radial basis functions with arbitrary derivatives at the R-matrix boundary is the key to the removal of this difficulty. Consequently the fact that we have actually found *smooth* behavior in the cross sections is strong evidence that there is indeed no resonant behavior.

The collisional pump mechanism for the cooling of the k doublets in H_2CO depends sensitively upon the state-to-state rate constants. These are obtained from the corresponding cross sections by Boltzmann averaging. The previously computed rate constants included the apparent resonances at 32.7 and 47.7 K. Since these rate constants are widely used, it is clear that they must now be redetermined. Tables of all the presently computed cross sections are available from the authors. Cross sections if needed in other energy ranges can be computed on request (to J.G.).

The present calculations were carried out using a separately computed set of radial basis functions for each $j\tau$ state of formaldehyde, i.e., 16 sets in all. In retrospect, it appears that this is something of an "overkill", and a less sophisticated effective Hamiltonian could have been used.

The accuracy of the calculations have been checked at intervals for individual partial waves at particular energies using the de Vogelaere method[23] for solving the coupled channel problem, with parameters set very tightly. This is computationally very expensive but, we believe, reliable. For $J = 1$, at least two significant figure agreement between the two methods was obtained. The worst case is $J = 0$, for which the maximum discrepancy in the partial cross section between the L^2 R-matrix and de Vogalaere methods is ~10%; most partial cross sections were accurate to 0.1%–1%. However it should be stressed that these cross sections contribute insignificantly to the total.

ACKNOWLEDGMENTS

The L^2 R-matrix program is written as a segment of the MOLSCAT programs of Sheldon Green, whom we thank for a copy of the source. We thank Jeremy Hutson of Cambridge University for useful discussions, and the Science and Engineering Research Council (U.K.) for a grant of computer time on the IBM machines at the Rutherford Laboratory.

[1] C. J. Bocchetta and J. Gerratt, J. Chem. Phys. **82**, 1351 (1985).
[2] J. Gerratt and I. D. L. Wilson, Proc. R. Soc. London Ser. A **372**, 219 (1980).
[3] C. J. Bocchetta and J. Gerratt, J. Chem. Phys. (to be submitted).
[4] C. J. Bocchetta, Ph.D. Thesis, University of Bristol, 1983.
[5] P. J. A. Buttle, Phys. Rev. **160**, 719 (1967).
[6] P. Palmer, B. Zuckerman, D. Buhl, and L. E. Snyder, Astrophys. J. **156**, L147 (1969).
[7] N. J. Evans II, B. Zuckerman, G. Morris, and T. Sato, Astrophys. J. **196**, 433 (1975).
[8] C. H. Townes and A. C. Cheung, Astrophys. J **157**, L103 (1969).
[9] B. J. Garrison, W. A. Lester, and W. H. Miller, J. Chem. Phys. **65**, 2193 (1976).

[10]G. Herzberg, *Infrared and Raman Spectra of Polyatomic Molecules* (Van Nostrand Reinhold, New York, 1945).
[11]C. H. Townes and A. L. Schawlow, *Microwave Spectroscopy* (McGraw–Hill, New York, 1975).
[12]A. S. Davydov, *Quantum Mechanics* (Pergamon, London, 1975).
[13]T. Oka, J. Phys. Soc. Jpn. **15**, 2274 (1960).
[14]A. M. Arthurs and A. Dalgarno, Proc. R. Soc. London Ser. A **256**, 540 (1960).
[15]*Handbook of Mathematical Functions*, edited by M. Abramowitz and Y. A. Stegun (Dover, New York, 1965).
[16]B. J. Garrison, W. A. Lester, and H. F. Schaefer III, J. Chem. Phys. **63**, 1449 (1975).
[17]B. J. Garrison, W. A. Lester, P. Siegbahn, and H. F. Schaefer III, J. Chem. Phys. **63**, 4167 (1975).
[18]C. Bloch, Nucl. Phys. **4**, 503 (1957).
[19]E. B. Stechel, R. B. Walker, and J. C. Light, J. Chem. Phys. **69**, 3518 (1978).
[20]L. J. Robertson, B.Sc. Thesis, University of Bristol, 1981.
[21]P. G. Burke and H. M. Schey, Phys. Rev. **126**, 147 (1962).
[22]H. Feschbach, Ann. Phys. **5**, 357 (1958).
[23]R. de Vogelaere, J. Res. Natl. Bur. Stand. **54**, 119 (1955).
[24]R. G. Gordon, in *Atomic and Molecular Scattering*, Methods in Computational Physics, Vol. **10**, edited by Alder, Fernbach, and Rotenberg (Academic, New York, 1971).